Defense Technical Information Center
Compilation Part Notice

ADP012545

TITLE: Interaction of Electron Vortices under the Influence of Background Vorticity Distribution

DISTRIBUTION: Approved for public release, distribution unlimited

This paper is part of the following report:

TITLE: Non-Neutral Plasma Physics 4. Workshop on Non-Neutral Plasmas [2001] Held in San Diego, California on 30 July-2 August 2001

To order the complete compilation report, use: ADA404831

The component part is provided here to allow users access to individually authored sections of proceedings, annals, symposia, etc. However, the component should be considered within the context of the overall compilation report and not as a stand-alone technical report.

The following component part numbers comprise the compilation report:
ADP012489 thru ADP012577

INTERACTION OF ELECTRON VORTICES UNDER THE INFLUENCE OF BACKGROUND VORTICITY DISTRIBUTION

Y. Kiwamoto, K. Ito, A. Sanpei, Y. Soga, T. Yuyama and T. Michishita

Department of Fundamental Sciences, Faculty of Integrated Human Studies, Kyoto University
Kyoto 606-8501, Japan

Abstract. We report experimental studies on vortex dynamics carried out recently in Kyoto University by using electron plasmas that are trapped in the Malmberg configuration with variety of initial configurations. This report includes (1) relaxation of many-clump dynamic states to "crystallization", (2) single clump dynamics in a background vorticity distribution, (3) two-clump interaction in a low-level background vorticity distribution, and (4) accelerated "crystallization" of three clumps in a background vorticity distribution. Details are provided in companion papers reported in this workshop.

INTRODUCTION

A set of equations that describe 2-dimensional (2D) motion of guiding centers of electrons transverse to the externally applied homogeneous magnetic field $B_0 = B_0\hat{z}$ are isomorphic to those of the 2D Euler fluid of non-charged particles [1,2]. The simple relation $\zeta = en/\varepsilon_0 B_0 = \omega_p^2/\omega_c$ between the electron density n and the vorticity $\zeta(x,y) = \zeta\hat{z} = \nabla \times v(x,y)$ substantially eases the diagnostics of the flow distribution with $v = E \times B_0/B_0^2 = \hat{z} \times \nabla\phi/B_0$ in the electron plasma. Here ω_p and ω_c are the local plasma and cyclotron frequency, respectively. Since the stream function ψ, defined by $v = \hat{z} \times \nabla\psi$, is related to potential distribution simply by $\phi = B_0\psi$, the electrostatic analysis is directly applicable to the flow dynamics [2-4].

The potential distribution $\phi(x,y)$ is obtained numerically from $n(x,y)$ that is determined experimentally by means of the 2D luminosity distribution $I(x,y)$ on charge-coupled-device (CCD) camera images [3,4]. This diagnostic includes dumping all electrons along the magnetic field lines to a surface coated with 20nm-thick-Aluminum that also serves to electronically determine the total charge of electrons $-eN$ [5]. The linear relationship has been demonstrated between $I(x,y)$ and the line-integrated electron density distribution $n(x,y)L = \int dz n(x,y,z)$ in a wide dynamic range of $1:3000$ with a high sensitivity of 1 count per 10 electrons [4]. In this experiment the potential

distribution of the trap is modified from the Penning-equilibrium configuration [6] to the Malmberg-trap configuration so as to minimize the variation of the axial length [7]. The typical length is $L = 235\,$mm over the cross section.
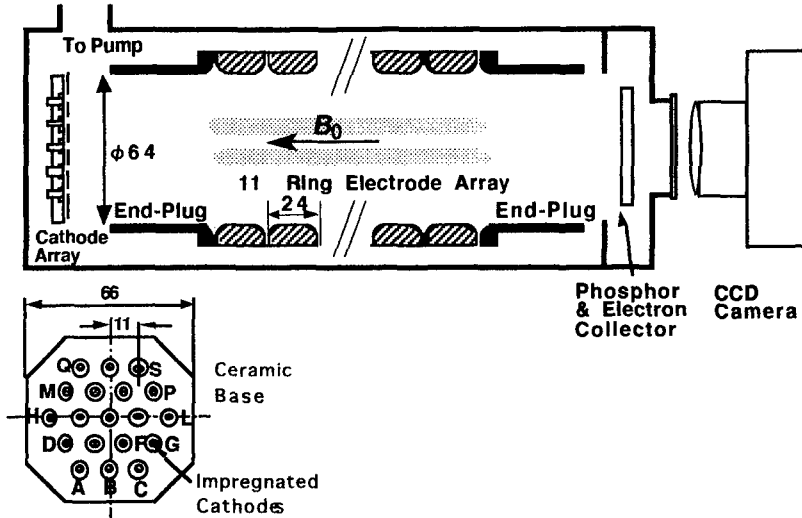

FIGURE 1. Schematic configuration of the experiment.

In the experimental setup as shown in Fig. 1 we use an array of 19 small electron emitters each of which can be operated independently to generate strings of electrons. Electrons in each string rotate around the string axis to form a vortex string with the initial diameter of $< 1\,$mm. The strings advect each other in a conducting cylindrical wall at 32mm from the machine axis. In addition to various configurations of electron strings (point vortices or clumps in 2D space), we can generate different shapes and levels of continuous vorticity distribution by combining repeated injection, mixing and relaxation of the strings and partially dumping electrons in the equilibrated distribution [5].

EXPERIMENTAL RESULTS

Relaxation of Many Vortex Strings to Crystal Structures

The most striking among the observations on vortex dynamics must be the formation of crystal states of vortices starting from spiral vorticity distribution that breaks apart into nearly a hundred of vortex strings [8]. Instead of relying on the instability process to generate the vortex strings we examine the dynamics by specifying the number of the strings as well as the position and circulation of each string. Even with highly reproducible initial distributions of the present experiment, the 19 vortices at maximum

go into random states of motion and repeat punctuated merging as well. During periods between intermittent merging, a decreasing number of vortex strings form regular arrays of "crystal" as illustrated in Fig. 2.
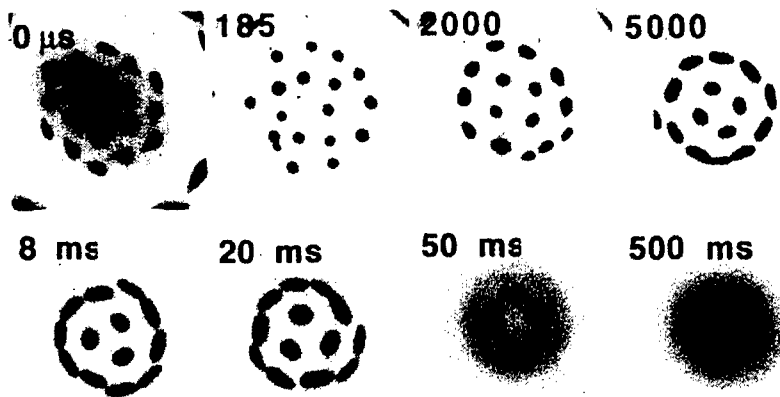

FIGURE 2. Time evolution of vorticity distribution starting from 19 clumps in vacuum.

In the process of the relaxation relatively weak strings are broken into thin sheets (filamented), and get folded into a stronger clump coming nearby. A noticeable process involved here is that some fraction of the sheets remains unabsorbed and forms a rugged background vorticity distribution. The self-generated background vortices significantly affect the process of interactions among remaining clumps. In this paper we focus on the role of the background vortices in the 2D dynamics of clumps that form various shapes of meta-equilibrium distribution as displayed in Fig. 3 in the relaxation process.
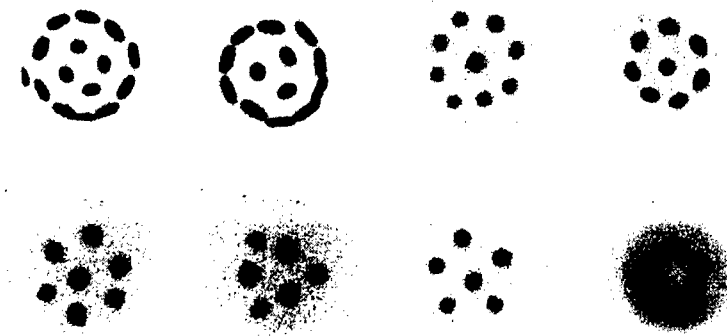

FIGURE 3. Meta-equilibrium vorticity distributions observed in the relaxation process. From [9,10].

Single Clump Dynamics in a Background Vortex

As a basic elementary process we examine the dynamics of a single vortex string in interaction with a background vortex with broad distribution. This configuration is also among well-discussed processes in planetary atmosphere, and qualitative behavior has been examined experimentally with normal fluids [11]. Quantitative examination became available only after Schecter and Dubin proposed a theoretical model based on the linearized equation of motion of the Euler fluid [12].
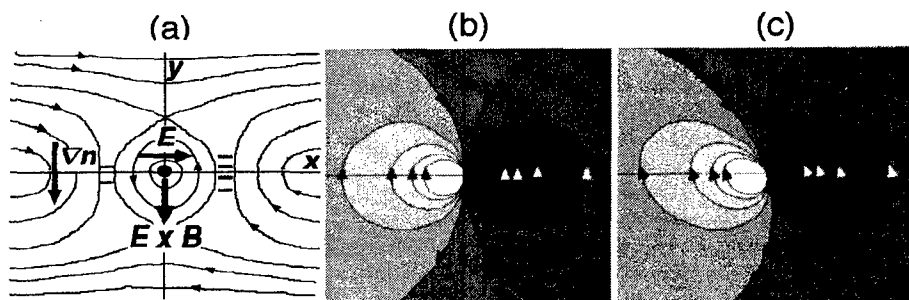

FIGURE 4. Perturbed vorticity distribution of the background in the slab model without shear (b) and with shear (c). The corresponding plasma distribution is shown in (a). From [5].

The velocity field of a clump, which is advected in the background vortex, locally modifies the latter's vorticity distribution ς_b if $\partial\varsigma_b/\partial r \neq 0$. In the rest frame of the clump, the higher (lower) vorticity of the background is moved to the lower (higher) region of ς_b, and the perturbation $\delta\varsigma_b$ forms a dipole structure aligned with the direction of the clump's motion as shown in Figs. 4 (b) and (c). In Fig. 4 ς_b increases downward while the clump moves to the left in the lab. frame. The solid curves in (b) and (c) stand for the contours of $\delta\varsigma_b$ as determined in the theoretical model with arrows indicating the direction of the advection. The dipole distribution of $\delta\varsigma_b$ generates a transverse velocity field at the center to drive the clump downward in the direction of increasing ς_b.

The experimentally determined vorticity distribution is plotted in Fig. 5 as a function of time in μs. The upper panel shows the total vorticity distribution $\varsigma = \varsigma_v + \varsigma_b$. The clump's distribution ς_v initially set at the periphery of the background vortex moves into the center of the background. The time required for this merging is within a couple of orbital rotation time. The perturbation $\Delta\varsigma = \varsigma - \varsigma_{b0}$ is determined by subtracting the initial background distribution ς_{b0} from each distribution in the upper panel and displayed in the lower panel. We can observe negative (positive) $\Delta\varsigma$ in front of

(behind) the clump in qualitative agreement with Figs. 4 (b)-(c) [5, 9, 10].
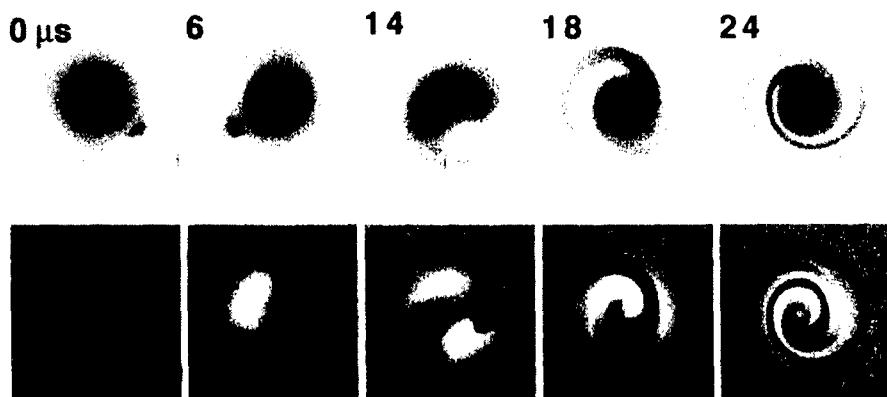

FIGURE 5. A clump climbs up the vorticity gradient of the background. The upper panels show the total vorticity while the lower panels present the increment $\Delta\varsigma$ of the vorticity from the initial distribution. Darkness represents the height of the vorticity. The white in the lower panels indicates negative $\Delta\varsigma$. From [9,10].

In the experiment, though the circulation Γ_v of clumps is less than a few percent of Γ_b of the background, the modification of the background distribution is substantially large and the perturbation does not remain local. If we decrease Γ_v, the clump is stretched into a filament by the shear in the background before it reaches the center. The radial distance r_v of the clump from the center of the vorticity distribution is plotted as a function of time in Fig. 6 for different values of $\Gamma_v \propto N_v/10^6$ $= (1.6\triangle, 4.4\square, 8.7\circ, 17\bullet)$ starting from the same radial location in the fixed profile of the background vorticity distribution. The clump begins its free motion at 15µs on disconnection from the electron source.
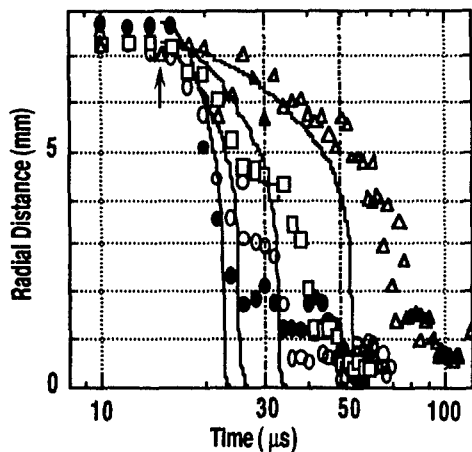

FIGURE 6. Radial distance of clumps with different circulations. From [5].

The solid curves stand for the radial distance as calculated from the Schecter's equation of motion by using the full experimental parameters of the initial distribution. Here we put the logarithmic factor $\ln(cr_v/\ell)$ in the equation to be 1. In the experiment the half-width $\ell = \left(\left|\Gamma_v/2\pi A\right|\right)^{1/2}$ of the separatrix reaches the radial distance r_v as the clump moves inward, and the logarithmic factor becomes zero indicating the breakdown of the slab-geometry approximation. If we do not drop the logarithmic factor and let the geometric coefficient $c = 1.5$, the calculated r_v does not decrease below 1mm (for small Γ_v) or 2mm (for large Γ_v). This cutoff distance of r_v qualitatively agrees with the radius where the orbit deviates from the initial path as observed in Fig. 6.

Avoiding the problems associated with the logarithmic factor, we examine the radial velocity of the clump along the initial trajectory of its motion. We compare the time required for the clump to travel from 10% to 90% point of the initial radial distance. The experimental value τ_{Exp} is evaluated by smoothly extrapolating the initial orbit below 3 mm. The corresponding theoretical value τ_{Model} is evaluated from the orbit calculated in the same manner as in Fig. 6. We have confirmed a clear scaling $\tau_{Exp} \approx 2\tau_{Model}$ for a wide range of experimental parameters [5]. This observation indicates the validity of the model equation as well as the necessity for more rigorous theoretical treatment in the range $cr_v/\ell \leq 1$. It should be noted also that the 2D field distribution $\phi(x,y)$, calculated numerically from the observed density distribution, predicts the $E \times B$ drift velocity of the clump that is consistent with the observed trajectories of the clumps for the whole radial range [13].

Two Clump Interaction in a Background Vortex

As an elementary process in the interaction among clumps, we examine trajectories of two clumps immersed in different levels of vorticity of the background. Example frames of the vorticity distribution are shown in Fig. 7. In contrast to the dynamics in vacuum, the two vortices approach in a time of a couple of rotations either to merge into one or to form a binary vortices. The binaries revolve stably at a distance of less than two vortex diameters at which they should get merged in vacuum [14].

Preliminary experiments carried out before the NNP workshop in 1999 have revealed that the time τ_{Merge} required for the merging or forming the binary state scales as $\propto \Gamma_b^{-k}$ with the exponent of $k = 0.8-1$ [15]. Assuming then unknown profile of the background as gaussian, the characteristic time scale of τ_{Merge} was approximated to τ_{Model} [16]. However, detailed experimental analyses carried out later with improved diagnostic technique have not led to a conclusion that τ_{Merge} show the same
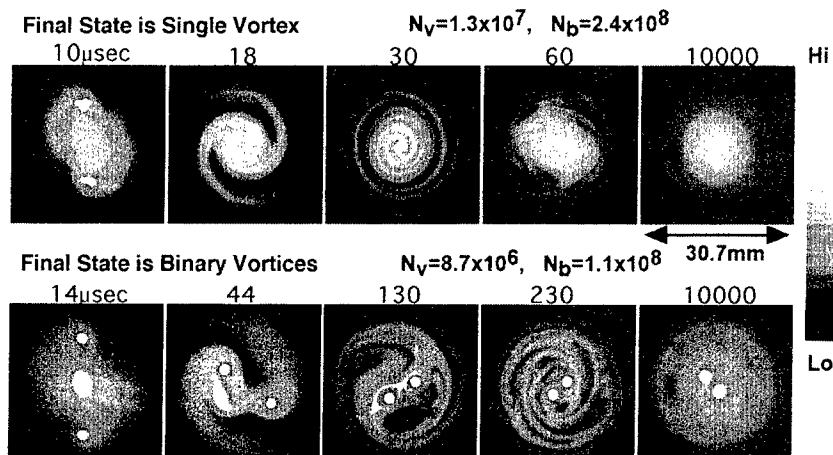
FIGURE 7. Time evolution of vortex dynamics including two clumps and background vortex.
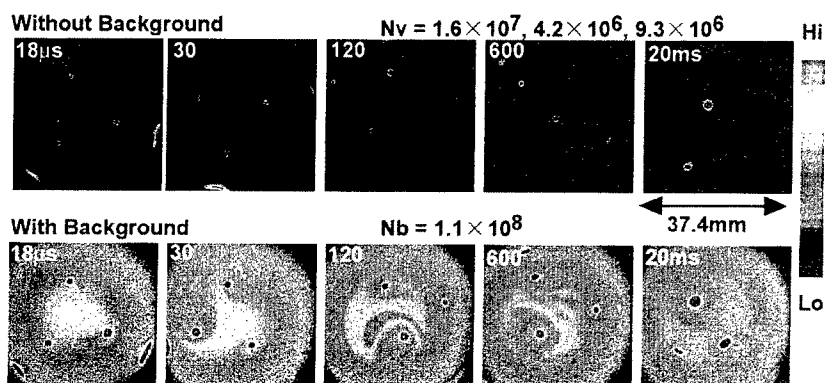

FIGURE 8. Three clumps of different strength are crystallized in the presence of a low-level background vorticity distribution.
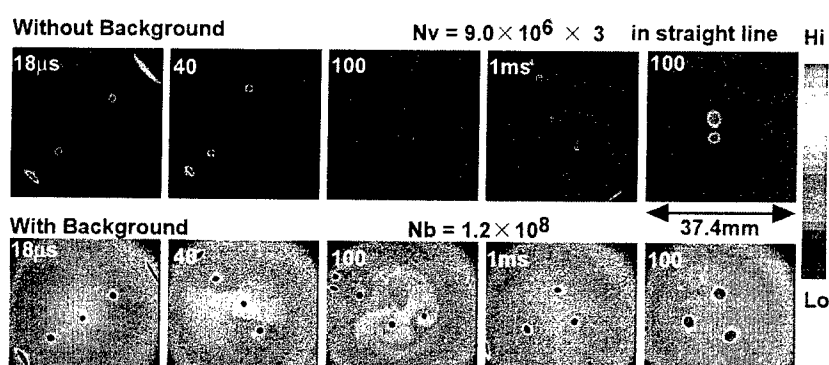

FIGURE 9. Three clumps in straight line are crystallized in the presence of a low-level background vorticity distribution.

parameter dependence as τ_{Model}.

Recent observations indicate that three vortices, two clumps plus a background vortex, almost equally take part in the evolution of the whole vortex dynamics. When the gradient of the background vorticity is large enough, the clumps quickly move up the hill of the background vorticity to merge around the background's peak. This is the case where the Schecter-Dubin model is the dominant process. When the background gradient is not large enough, however, the clumps modify the background locally first to form structures that surround them. The fine structures dressed by the clumps exert strong influence on the interaction between the clumps as well as between each clump and the remaining part of the background vortex. In these processes various shapes of areas with depleted vorticity (patched holes accompanying the clumps and ring holes surrounding them) are generated [3,9,10,17]. The difference in the initial conditions, separating the fates of the vortex dynamics is quite subtle.

Crystallization of Three Clumps in a Background Vortex

At least three clumps may be required to test crystallization of discrete vortices in the simplest form. When three clumps are placed at the vertices of a regular triangle in vacuum, they keep the relative location unchanged in a rigidly rotating frame only if the initial distribution is highly symmetric. If the symmetry is broken in terms of the relative positions or by the imbalance of the circulations, the clumps continue unsettled motion until non-ideal processes set in or one of them moves out to touch the wall.

As in the case of two clump dynamics, the presence of a low level background vortex changes the dynamical state drastically. Figure 8 shows how the initial distribution of symmetrically placed clumps with uneven circulations $\Gamma_v \propto N_v/10^6 = (16, 9.3, 4.2)$ evolves in vacuum (upper panels) and in the presence of the background vortex with $\Gamma_b \propto N_b/10^8 = 1.1$ (lower panels). The clumps start free motion at $t = 18\mu s$ as indicated at the upper left corner. It is clearly observed that the symmetric layout of the clumps is lost in a couple of rotation times in vacuum. The center of mass (CM) of the three-clump system also rotates indefinitely. When a background vortex is added, the clumps are forced to remain at azimuthally symmetric positions and the radial excursion of the CM decreases substantially.

The differences from the vacuum dynamics are associated with modifications of the background distribution. The average height of the background distribution is lower than those of the clumps by a factor of 14-60, and the background distribution is locally modified around each clump as soon as the free motion sets in. The extent of the modification differs for different strengths of clumps as evidently observed in the lower panels at $t = 20\text{-}600\mu s$. The radial extent of the modified distribution is larger for the stronger clump. Typical states of meta-equilibrium are associated with a ring hole

around the clumps as observed in the lower panel at $t = 20$ms.

The triangular distribution in meta-equilibrium states of three clumps is realized even from initial states far from the final configurations. Figure 9 shows that the clumps initially placed in a straight line also form a robust triangular configuration after experiencing interactions with the background vortex. The background vorticity distribution restricts excursion of the clumps within a limited area and let the clumps settle at triangular vertices and finally prevent them from merging. The responsible dynamics of the background vortex for this crystallization appears to be the deformation of its distribution agitated in the relatively strong field of each clump. The net field of each clump tends to get equalized, but not fully, by the shielding dress of the modified distribution of the background vortex.

DISCUSSION AND CONCLUSIONS

In this paper we have examined the role of the background vorticity distribution that exerts a decisive influence on the 2D dynamics of clumps. The vorticity gradient in the background tend to advect the clumps to climb the slope. But in most actual situations the reaction from the clumps is so substantial that various shapes and scales of structures are generated in the background distribution. Such structures in turn remarkably modify the interaction among clumps so that they find relative positions which lasts for as long a period as exceeding 100 rotations. These stable states of meta-equilibrium are responsible for the formation of vortex crystals.

Ring holes are generated around the clumps with different sizes corresponding to the circulations of the clumps (see Fig. 8). Coulomb shielding by the holes is requested in the statistical model of the crystallization[18]. Our observations indicates that the amount of the negative circulations of the ring holes do not exceed 20 % of the clumps and usually remain below a few percent. [17]

The time required for three clumps to form a meta-equilibrium triangle decreases as the height of the background vorticity increases. Observations indicates that there is no threshold for the accelerated crystallization in the background level that separates from the dynamic states in the vacuum. We have confirmed such continuous transitions by decreasing the height of the background vorticity well below 0.05% of the clumps' local vorticity [19]. The tendency of saturation has also been observed that the crystallization time does not decrease to less than a couple of rotation times as the background level increases above 1% of the clumps'.

Our experimental investigations indicate that fates of the dynamics of interacting clumps are sensitively influenced through the interaction with a low level distribution of the vortex that surrounds them. However, we have not reached a satisfactory explanation in terms of existing statistical models. From experimental point of view the deformations of the holes appear to be essential for meta-equilibration of the clumps'

configuration, namely the apparently static state is supported by fine-scale dynamics.

We tend to understand the phenomena as follows: In the meta-equilibrium states of the clumps, the background vortex has rugged distribution with fine structures and remains in a dynamic state, continuously adjusting its spatial profile with incompressible fine-scale flows along intricate paths. When the background dynamics becomes unable to sustain the force balance among the clumps, merging between clumps occurs in a short period to form another meta-equilibrium distribution with reduced number of clumps. The crystallized distributions as shown in Fig. 2 manifest such states punctuated by the intermittent merging.

ACKNOWLEDGMENTS

REFERENCES

1. Levy, R. H., Phys. Fluids **11**, 920 (1968).
2. Fine, K. S., Driscoll, C. D., Malmberg, J. H., and Mitchell, T. B., Phys. Rev. Lett. **67**, 588 (1991).
3. Huang, X. -P., Fine, K. S., and Driscoll, C. F., Phys. Rev. Lett. **74**, 4424 (1995).
4. Ito, K., Kiwamoto, Y., Sanpei, A., Jpn. J. Appl. Phys. **40**, 2558 (2001).
5. Kiwamoto, Y., Ito, K., Sanpei, A., Mohri, Phys. Rev. Lett. **85**, 3173 (2000).
6. Higaki, H. and Mohri, A., Jpn. J. Appl. Phys. **36**, 5300 (1997).
7. Finn., J. M., del Castillo-Negrete, D., and Banes, D. C., Phys. Plasmas **6**, 3744 (1999).
8. Fine, K. S., Cass, A. C., Flynn, W. G., Driscoll, C. F., Phys. Rev. Lett. **75**, 3277 (1995).
9. Kiwamoto, Y., *BUTSURI* (Bull. Phys. Soc. Jpn.) **56**, 253 (2001).
10. Kiwamoto, Y., J. Plasma Fusion Research **77**, 338 (2001).
11. Nezlin, M. V., and Snezhkin, E. N., *Rossby Vortices, Spiral Structures, Solitons,* Springer-Verlag, Berlin Heidelberg, 1993.
12. Schecter, D. A., and Dubin, H. E., Phys. Rev. Lett. **83**, 2191 (1999).
13. Ito, K., Kiwamoto, Y., Sanpei, A., to be published; also partly reported in this workshop.
14. Mitchell, T. B., Driscoll, C. D., and Fine, K. S., Phys. Rev. Lett. **71**, 1371 (1993).
15. Kiwamoto, Y., Mohri, A., Ito, K., Sanpei, A., and Yuyama, T., *Non-neutral Plasma Physics* III ed. by J. Bollinger, R. L. Spencer, R. C. Davidson, AIP Conf. Proc. 498, 1999, pp.99-105.
16. Kiwamoto, Y., Ito, K., Sanpei, A., Mohri, A., Yuyama, T., Michishita,T., J. Phys. Soc. Jpn. (Lett.) **68**, 3766 (1999).
17. Sanpei, A., Kiwamoto, Y., Ito, K., J. Phys. Soc. Jpn. (Lett.) **70**, No.10 (2001).
18. Jin, D. Z. and Dubin, D. H. E., Phys. Rev. Lett. **80**, 4434 (1998).
19. Sanpei, A., Kiwamoto, Y., Ito, K., Soga, Y., to be published; also partly reported in this workshop.